Monopole and quadrupole polarization effects on the α-particle description of ^{8}Be

A. Sytcheva, F. Arickx, and J. Broeckhove
University of Antwerp, Antwerpen, B2020, Belgium

V. S. Vasilevsky
Bogolyubov Institute for Theoretical Physics, Kiev, 03143, Ukraine

(Received 24 November 2004; published 29 April 2005)

We investigate the effect of monopole and quadrupole modes on the elastic α-α resonance structure of ^{8}Be. To this end, we make a fully microscopic coupled-channels calculation with three coupled channels, using the algebraic model. The continuum spectrum and wave functions are analyzed in terms of the individual channels to understand the nature of the resonances. It is shown that both monopole and quadrupole modes have a nonnegligible effect on the resonances in the α-α continuum.

DOI: 10.1103/PhysRevC.71.044322 PACS number(s): 21.60.Gx, 21.60.Ev, 24.30.Gd, 25.55.Ci

I. INTRODUCTION

^{8}Be is known to be a strongly clustered nucleus that appears through relatively short-lived resonances just above the α-α scattering threshold. A low-lying rotational band is experimentally apparent and suggests a strong deformation of the eight-particle resonance system. A systematic survey of the full spectrum of ^{8}Be, including a review of available theoretical and experimental results, has been made in the work of Ajzenberg-Selove [1] and is now available in a revised version [2]. Bacher *et al*. [3] have reported partial phase shifts in the α-α collisions for even states up to $L = 6$ in the range up to 35 MeV excitation energy. Together with [4], these experiments reveal no resonance states with measurable widths between 25 and 50 MeV in the elastic α-α channel. Arena *et al*. [5] point out the need for including inelastic channels such as ^{4}He(^{4}He,d)^{6}Li, ^{4}He(^{4}He,n)^{7}Be, and ^{4}He(^{4}He,p)^{7}Li if one wants to find states of high excitation energy. These authors report the possible existence of highly excited ^{8}Be levels for $L = 6$ and $L = 12$ at about 41 MeV and $E_x = 43$, and around 50 MeV for $L = 2$ up to $L = 10$.

Because of the strong experimental evidence for the predominance of cluster structure in ^{8}Be, many theoretical approaches based on cluster structures have been considered. Microscopic cluster models are known to provide valuable information about the structure of light nuclei [6,7] and in particular of ^{8}Be. The resonating group method (RGM) has often been used [8–11]. The low-lying rotational structure of ^{8}Be, both in position and width, is reproduced by elastic α-α scattering calculations with effective interactions. The Coulomb interaction plays an important role in the correct position and width of these states, in particular for the $L = 0$ ground state of ^{8}Be [12,13].

Collective A-particle deformation models for light nuclei have been under discussion for several decades. A meaningful classification scheme has been derived for such models through the irreducible representations of the noncompact Sp(2,R) group. A good description of the low-energy spectra of light nuclei [14] and more specifically of the rotational structure of ^{8}Be [15] has been obtained within these models. It has also been demonstrated that the quadrupole Sp(2,R) model of ^{8}Be and the α-particle description have an important overlap and thus are complementary in the description of this nucleus [16], a conclusion confirmed in [17–19]. It seems, therefore, appropriate to study the coexistence and competition between collectivity and clustering in light nuclei through a combined approach. Filippov *et al*. [20–22] have already investigated cluster-monopole and cluster-quadrupole descriptions of ^{8}Be. Furthermore, the deformation aspect in ^{8}Be has been studied within a cluster approach by introducing a quadrupolar polarization of the α particles [23] or a monopolar distortion of the α particles [24].

In this work we propose a model in which the α-particle description and the collective (eight-particle) quadrupole and monopole modes are coupled. We consider a scattering approach within an energy range in which the α-cluster channel is open and both collective channels are closed, thus limiting ourselves to the elastic α-α cluster decay. The effects of the collective channels will then only be apparent in the compound system during resonance lifetimes.

The coupled-channels calculation follows the modified J-matrix method (MJM) [25,26], which is an extension of the J-matrix method (JM) [27] and is also known as the algebraic model [28,29]. The method is particularly suitable for situations that involve both bound and continuum states. It uses an oscillator expansion for the formulation of the Schrödinger equation and maps the bound-state and scattering boundary conditions from configuration space to the space of expansion coefficients. An important feature of the resulting equations is that the kinetic energy, i.e., the free space Hamiltonian, has a tridiagonal representation. That feature makes it possible to derive the free asymptotic states in the expansion coefficient representation. One solves the scattering equations in terms of a phase shift by matching the solution of the Schrödinger matrix equation to these asymptotic states at the boundary of what is considered to be the internal region. The MJM even allows one to treat long-range interactions, including the Coulomb potential, in the oscillator basis. It provides convergence in terms of number of basis functions with reasonable basis sizes, which is important because the

calculation of Hamiltonian matrix elements is the bulk of the method's computational load. The choice of an oscillator basis also provides for an easy calculation of Gaussian operators.

The multichannel approach of this work allows a clear-cut analysis of the elastic α-α phase shifts and corresponding wave functions in terms of the contribution from the individual channels, leading to a physical interpretation of the resonances. It indicates the importance of collective degrees of freedom in the compound system.

Our approach is most suited to handling two-body Gaussian interactions, mainly because of the oscillator expansion in the MJM. We consider two-body potentials—such as the one proposed in [30] and determined within a Hartree-Fock approximation and the ones from [31,32] determined within an RGM approach—to calculate the ^{8}Be spectrum and to check the validity of our conclusions.

The paper is organized as follows. In Sec. II we elaborate on the combined cluster-collective model description for ^{8}Be and formulate the multichannel MJM scattering approach. In Sec. III we discuss the numerical application of the MJM and present the results of the three-channel calculation. Section IV is devoted to the analysis of the results of the previous section in terms of contributions from the individual channels. Concluding remarks are presented in Sec. V.

II. A COUPLED-CHANNELS CLUSTER-COLLECTIVE MODIFIED *J*-MATRIX APPROACH

The modified *J*-matrix method [25,26], also referred to as the algebraic version of the RGM [29], has become a well-tested approach for nuclear structure calculations involving multichannel cluster and/or collective descriptions for light nuclei. The application of the MJM is based on an expansion in terms of oscillator basis states in the respective collective coordinates (intercluster distance, monopole radius, quadrupole deformation, etc.). We refer to the papers of Vasilevsky *et al.* [33–36] for detailed properties of the individual channel wave functions and to the multichannel formulation of the MJM [37] with nonorthogonal bases.

The model considered here for ^{8}Be consists of a wave function containing three structure components distinguished by a specific collective coordinate. These three components represent the α-α cluster, the Sp(2,*R*) quadrupole and the Sp(2,*R*) monopole modes

$$\Psi = \Psi^C + \Psi^Q + \Psi^M. \tag{1}$$

The structure of a single cluster is described by the wave function

$$\Psi_i(\alpha_i) = \Psi_i\left(\mathbf{q}_1^{(i)}, \mathbf{q}_2^{(i)}, \mathbf{q}_3^{(i)}\right), \qquad i = 1, 2, \tag{2}$$

centered around its center of mass $\mathbf{R}_i$. A two-cluster wave function can then be written as

$$\Psi^C(\mathbf{q}_1, \ldots, \mathbf{q}_7) = \mathcal{A}\left[\Psi_1(\alpha_1)\,\Psi_2(\alpha_2)\;\Psi_R(\mathbf{r})\right], \tag{3}$$

where $\mathcal{A}$ stands for the antisymmetrization operator over all eight particles, and $\Psi_R(\mathbf{r})$ represents the relative motion of both clusters, $\mathbf{r}$ being the corresponding Jacobi coordinate.

To limit the computational complexity of the problem, the cluster wave functions are frozen and constructed as Slater determinants of harmonic oscillator ($0s$) states, corresponding to the ground-state shell-model configuration of the cluster. The $\Psi_R(\mathbf{r})$ wave function for the relative motion will be represented by an expansion in terms of an oscillator basis in $\mathbf{r}$. As the cluster states are frozen and built of ($0s$) orbitals, the quantum numbers reduce to those of the intercluster wave function only. The set of quantum numbers is unambiguously defined and obtained from the reduction of the symmetry group $U(3) \supset O(3)$ of the one-dimensional oscillator. This reduction provides the quantum numbers n for the radial excitation, and L, M for the angular momentum of the two-cluster system. The two-cluster wave function can be decomposed as

$$\begin{aligned}\Psi^C_{LM} &= \mathcal{A}\left[\Psi_1(\alpha_1)\,\Psi_2(\alpha_2)\,\Psi_{LM}(\mathbf{r})\right] \\ &= \sum_n c^C_{nL}\mathcal{A}\left[\Psi_1(\alpha_1)\;\Psi_2(\alpha_2)\,\phi_{nLM}(\mathbf{r})\right] = \sum_n c^C_{nL}\psi^C_{nLM},\end{aligned} \tag{4}$$

where the $\phi_{nLM}(\mathbf{r})$ are the three-dimensional harmonic oscillator states. The oscillator parameter b is the same for both the individual particle ($0s$) states and the expansion for the relative motion.

The oscillator decomposition of collective Sp(2,*R*) quadrupole and monopole components are most easily introduced through the standard step operators

$$\Psi^Q_{LM} = \sum_n c^Q_{nLM} N^{(Q)}_{LM} P_{LM}\left[A^+_Q\right]^n \Phi_0 = \sum_n c^Q_{nLM}\psi^Q_{nLM}, \tag{5}$$

$$\Psi^M_{LM} = \sum_n c^M_{nL0} N^{(M)}_{LM}\left[A^+_M\right]^n P_{LM}\Phi_0 = \sum_n c^M_{nLM}\psi^M_{nLM}, \tag{6}$$

where Φ_0 is a $0\hbar\omega$ shell-model vacuum state. For ^{8}Be this is a Slater determinant with a $(0s)^4(0p)^4 = (000)^4(001)^4$ configuration [in Cartesian (n_x, n_y, n_z) oscillator notation], and it has SU(3) $(\lambda, \mu) = (40)$ classification. The P_{LM} stands for the traditional angular momentum projection operator, and $N^{(M)}_{LM}$, $N^{(Q)}_{LM}$ are norm factors. The (translationally invariant) step operators $A^+_{\mu\nu}$ in a Cartesian notation ($\mu, \nu = x, y, z$) are written in terms of the standard harmonic oscillator creation operators $a^+_\mu(i)$ for particle i as

$$A^+_{\mu\nu} = \sum_{i=1}^{A} a^+_\mu(i)a^+_\nu(i) - \frac{1}{A}\sum_{i,j=1}^{A} a^+_\mu(i)a^+_\nu(j), \tag{7}$$

so that

$$\begin{aligned}A^+_Q &= A^+_{zz}, \\ A^+_M, &= A^+_{xx} + A^+_{yy} + A^+_{zz}.\end{aligned} \tag{8}$$

The projection after excitation for the quadrupole mode in (5) is necessary because the step operator A^+_Q contains both $L = 0$ and $L = 2$ components. In the monopole case, the projection operator commutes with the step operators. A single projection of the $0\hbar\omega$ state, which contains $L = 0, 2$, and 4 components, suffices. Thus, the monopole mode contributes only to those L subspaces. Contrary to the cluster

and quadrupole modes, this limits the monopole Hilbert space to the latter angular momenta. We will therefore limit ourselves to $L = 0, 2$, and 4 for all modes throughout this work.

We use the same oscillator parameter b for Ψ^Q_{LM} and Ψ^M_{LM} functions as we do for the cluster wave function Ψ^C_{LM}. This makes the calculation of overlap and Hamiltonian matrix elements significantly easier.

One has, of course, orthogonality with respect to the quantum numbers (n, L, M), but not with respect to the channel label:

$$\left\langle \psi^{\tau}_{nLM} \middle| \psi^{\upsilon}_{n'L'M'} \right\rangle \sim \delta_{n,n'}\delta_{L,L'}\delta_{M,M'}, \tag{9}$$

where τ and υ stand for the cluster C, monopole M, and quadrupole Q channels. In particular, it is well known [16] that with a common choice of overall b, the $n = 0$ basis states of all modes are identical:

$$\psi^C_{0LM} = \psi^Q_{0LM} = \psi^M_{0LM}. \tag{10}$$

This means that care should be taken in the interpretation of the results when attributing an effect to some channel or other.

The calculation of overlap and Hamiltonian matrix elements is most easily performed by considering Gaussian-type generating functions for the three oscillator expansions, which are (up to L projection)

$$\begin{aligned}
\psi^C(\mathbf{R}) &= \mathcal{A}[\Psi_1(A_1)\,\Psi_2(A_2)\phi(\mathbf{r}|R)] \\
&= \mathcal{A}\Bigg[\Psi_1(A_1)\Psi_2(A_2)\exp\left\{-\frac{1}{2b^2}\mathbf{r}^2 + \frac{\sqrt{2}}{b^2}(\mathbf{R}r) - \frac{1}{2b^2}\mathbf{R}^2\right\}\Bigg] \\
&= \mathcal{A}\left[\Psi_1(A_1)\Psi_2(A_2)\exp\left\{\left(\mathbf{R}\bullet A^+_C\right)\right\} \times \exp\left\{-\frac{1}{2b^2}\mathbf{r}^2\right\}\right], \\
\psi^Q(\epsilon) &= \exp\left\{\epsilon A^+_Q\right\}\Phi_0, \\
\psi^M(\upsilon) &= \exp\left\{\upsilon A^+_M\right\}\Phi_0,
\end{aligned} \tag{11}$$

where we introduced the step operator $\mathbf{A}^+_C = \mathbf{a}^+(\mathbf{r})$ for the oscillator decomposition of the cluster wave function.

Because of the Gaussian nature of the generating functions, matrix elements for the overlaps and Gaussian two-body operators can be calculated in a straightforward way. From these, the matrix elements in the discrete (n, L, M) basis can then be obtained by, e.g., recurrence techniques [29,37].

By substituting the expansions (4)–(6) as an ansatz for the solution (1) in the Schrödinger equation, the latter reduces to an infinite matrix equation to be solved for the coefficients c^C_{nL}, c^Q_{nL}, and c^M_{nL}:

$$\sum_{\tau'}\sum_{m}\langle nL,\tau|\hat{H} - E|mL,\tau'\rangle c^{\tau'}_{mL} = 0. \tag{12}$$

We solve this equation by considering the modified J-matrix approach, which was formulated in terms of an oscillator decomposition of the trial solution and provides fast convergence in a finite subset of the model subspace. In the J-matrix approach, the boundary conditions (for scattering as well as bound-state solutions) are translated from coordinate into the space of basis expansion coefficients, and asymptotic solutions can be obtained from a three-term recurrence relation for the expansion coefficients for high n. After setting the coefficients to equal the asymptotic values from a given $n = N$ on and imposing a matching condition between the interaction region and asymptotic regions, only a reasonably sized matrix equation remains to be solved. In the modified J-matrix approach, asymptotic contributions for the potential behavior, in particular for the Coulomb term, are taken into account in a semiclassical way through a modified recurrence equation. This was shown to drastically reduce the size N of the remaining matrix equation.

For the scattering boundary condition, the asymptotic regular $c^{(+)}_{nL}$ and irregular $c^{(-)}_{nL}$ solutions are obtained so that the asymptotic expansion coefficients of the solution can be written as

$$c^{as}_{nL} \to c^{(-)}_{nL}(kR_{n,l}) - Sc^{(+)}_{nL}(kR_{n,l}), \qquad n \to \infty, \tag{13}$$

where S stands for the S matrix and reflects the matching condition. It is to be determined by solving the remaining matrix equation. $k = \sqrt{2mE/\hbar^2}$ is the momentum corresponding to energy E, and $R_{n,l}$ are the oscillator turning points for the channel under consideration. In a single-channel approach, S is a scalar quantity related only to the phase shift.

For the bound-state boundary condition, only the exponentially decaying solution can be retained, and its expansion coefficients are

$$c^{as}_{nL} \to \exp(-\varkappa R_{n,l})/\sqrt{R_{n,l}}, \qquad n \to \infty, \tag{14}$$

with $\varkappa = \sqrt{2m|E|/\hbar^2}$. In (13) and (14), energy E is determined with respect to the threshold of the corresponding channels.

In our approach, we have three different channels, so a multichannel MJM formulation is necessary. We take the same form as in [35] and write

$$c^{\tau}_{nL} = c^{(0)\tau}_{nL} + \delta_{\upsilon\tau}c^{(-)\tau}_{nL} - S_{\upsilon\tau}c^{(+)\tau}_{nL}, \tag{15}$$

with υ the entrance channel, and τ any other coupled channel. Substitution of (15) in the matrix form of the Schrödinger

TABLE I. Parameters used for Minnesota (Mi), Volkov (V1), and modified Hasegawa-Nagata (MHN) potentials and corresponding cluster and quadrupole threshold energies with respect to the monopole breakup energy.

	Mi	V1	MHN
Original Majorana parameter	0.52	0.6	0.39
Modified Majorana parameter	0.57	0.6	0.43
Oscillator parameter b (fm)	1.28	1.37	1.32
$E_{\text{g.s.}}$ of ^{4}He, MeV	−24.69	−27.09	−29.01
$E_{\text{th}}(C)$, MeV	−49.37	−54.17	−58.02
$E_{\text{th}}(M)$, MeV	0.0	0.0	0.0
$E_{\text{th}}(Q)$, MeV	39.22	23.16	25.28

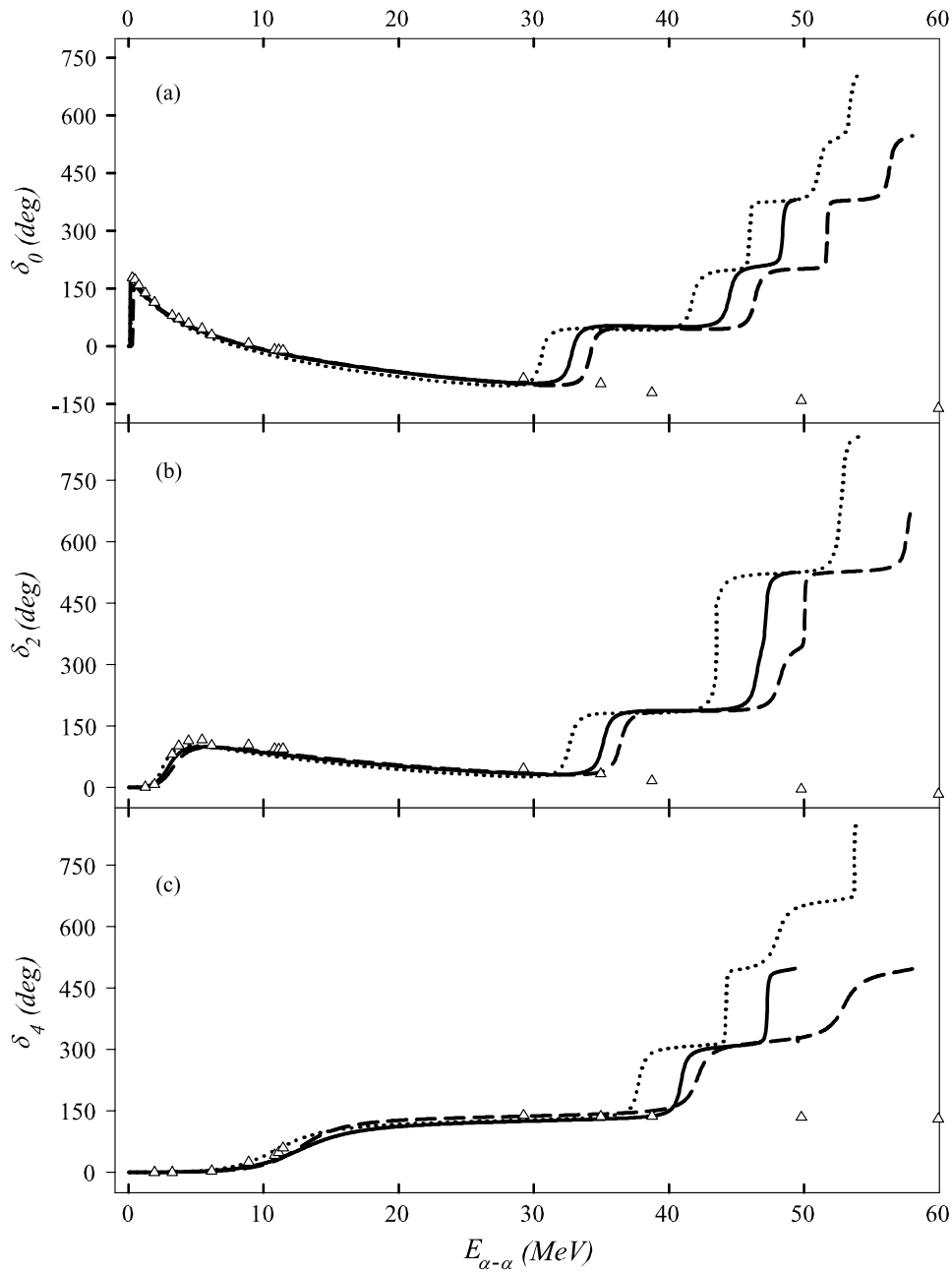

FIG. 1. Phase shifts obtained in the multichannel MJM approach with Minnesota (solid), Volkov (dotted), or MHN (dashed) forces for $L = 0$ (a), $L = 2$ (b), and $L = 4$ (c). Triangles indicate experimental data from [3,4]. $E_{\alpha\text{-}\alpha}$ is the c.m. energy with respect to the cluster threshold.

equation leads to

$$\sum_{\tau'}\sum_{m<N}\langle nL,\tau|\hat{H}-E|mL,\tau'\rangle c_{mL}^{(0)\tau'} - \sum_{\tau'} S_{\upsilon\tau'}\left[\beta_0^{(+)\tau'}\delta_{n,0}\delta_{\tau'\tau}+V_n^{(+)\tau\tau'}\right] = -\beta_0^{(-)\tau}\delta_{n,0}\delta_{\upsilon\tau}-V_n^{(-)\tau\upsilon} \tag{16}$$

and

$$V_n^{(\pm)\tau\tau'}=\sum_{m=0}^{\infty}\langle nL,\tau|\hat{V}|mL,\tau'\rangle c_m^{(\pm)\tau'}, \tag{17}$$

where $\hat{V}$ stands for the two-body interaction and β_0 accounts for the traditional regularization of the irregular asymptotic solution (see for instance [29] or [35]).

This system of equations should then be solved for the residual coefficients $c_{nL}^{(0)\tau}$ and the S-matrix elements $S_{\tau\tau\prime}$. We consider in Eqs. (16) and (17) a near-interaction region with $n < N$ and a far-interaction region with $n \geqslant N$. The choice of N is such that one can expect the residual expansion coefficients $\{c_{nL}^{(0)\tau}\}$ to be negligibly small in the far-interaction region. The total number of equations for a given entrance channel υ then equals to $N_{\rm ch}(N+1)$, and solving the set of equations by traditional numerical linear algebra leads to the $N_{\rm ch}N$ residual coefficients $\{c_n^{(0)\tau};\ \tau = C, Q, M;\ n = 0,\ldots,N-1\}$ and $N_{\rm ch}$

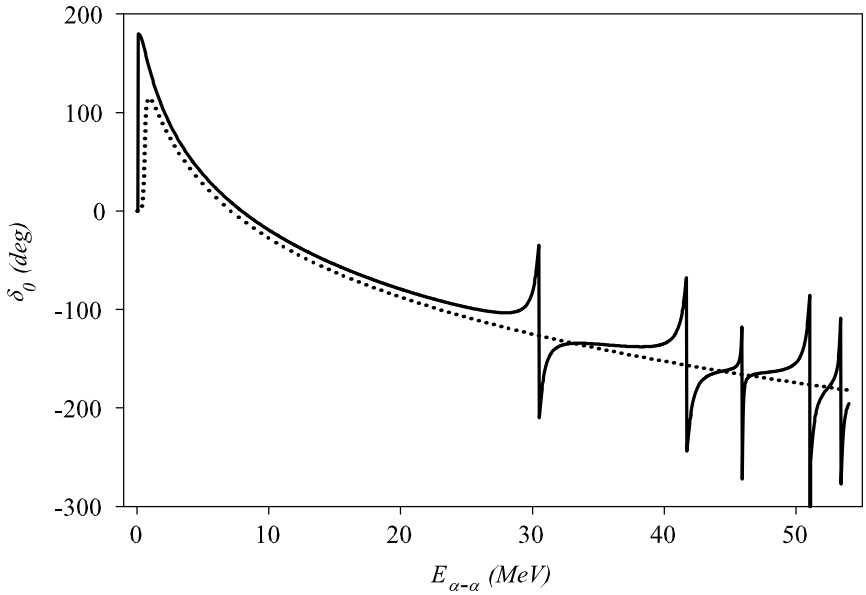

FIG. 2. $L = 0$ phase shifts for the Volkov potential in the one-channel cluster (dotted) and three-channel cluster-collective (solid line) approach. $E_{\alpha\text{-}\alpha}$ is the c.m. energy with respect to the cluster threshold.

S-matrix elements $\{S_{\upsilon\tau};\ \tau = C, Q, M\}$. The set of equations has to be solved for all $N_{\rm ch}$ entrance channels. A final parameter of the calculation concerns the summation in (17). Because the potential matrix elements decrease rapidly when $|n - m|$ gets large, we can truncate this sum at some $M > N$.

In this paper, we limit ourselves to the situation in which only the cluster channel is open, so that $\upsilon = C$, because this is the dominant channel for ^{8}Be in our model description. The boundary conditions (13) are appropriate for an open channel and are therefore used for the cluster channel; conditions (14) are appropriate for a closed channel and are thus applied to the monopole and quadrupole channels. This choice limits the energy range between the monopole threshold at 0 MeV (all eight particles infinitely apart) and the cluster threshold. The quadrupole threshold is even higher, because of the forced polarization condition.

III. NUMERICAL APPLICATION AND RESULTS

In a microscopic calculation, the choice of the effective nucleon-nucleon (*NN*) interaction remains a crucial point. We limit ourselves to effective *NN* interactions of Gaussian form, which lead to a straightforward evaluation of matrix elements in the cluster-collective model space. One well-known example is the Volkov [30] force, which was essentially determined and used within a Hartree-Fock context. This force binds both the deuteron triplet and the dinucleon singlet. Gaussian forces that discriminate between the deuteron singlet and dinucleon triplet are the Minnesota [31] and the Hasegawa-Nagata [38,39] potentials. A modified version of the latter was proposed in [32]. These interactions were considered and tested in α-N and α-α RGM scattering calculations.

In the current calculations, we consider the Volkov (V1), modified Hasegawa-Nagata (MHN), and Minnesota (Mi) forces. We include the Coulomb interaction, which is necessary to produce the $L = 0$ ground state as a narrow resonance just above the α-α threshold. The parameters are chosen to reproduce both the ground-state energy and size of ^{4}He. The Majorana exchange part accounts for nuclear matter properties. It does not influence the ground-state energy and size of ^{4}He, but it does affect the deformation in p-shell nuclei significantly [31].

To obtain the phase shifts for elastic α-α scattering, we solve (16) and determine resonance positions and widths in

TABLE II. Resonance energies and widths in the coupled-channel calculation for Minnesota (Mi), Volkov (V1) and modified Hasegawa-Nagata (MHN) potentials. Resonance energies are in MeV, widths in keV.

	Mi		V1		MHN	
	E_r	Γ	E_r	Γ	E_r	Γ
0_1^+	0.120	195	0.090	1910	0.085	0.2
0_2^+	32.78	823	30.51	761	33.78	827
0_3^+	44.45	762	41.72	843	46.04	876
0_4^+	48.41	208	45.92	95	51.42	76
0_5^+	x	x	51.06	616	56.08	618
0_6^+	x	x	53.41	285	x	x
2_1^+	2.94	2126	2.56	1679	2.98	1712
2_2^+	35.13	8418	32.59	7977	36.08	1052
2_3^+	46.51	636	43.48	949	47.90	1128
2_4^+	47.17	235	44.48	0.2	49.69	80
2_5^+	x	x	52.84	250	57.40	554
4_1^+	12.63	7799	10.81	6705	12.07	4241
4_2^+	40.89	656	37.75	674	41.85	1514
4_3^+	47.26	127	44.17	83	49.03	20
4_4^+	x	x	48.01	1129	52.64	2011
4_5^+	x	x	53.68	67	x	x

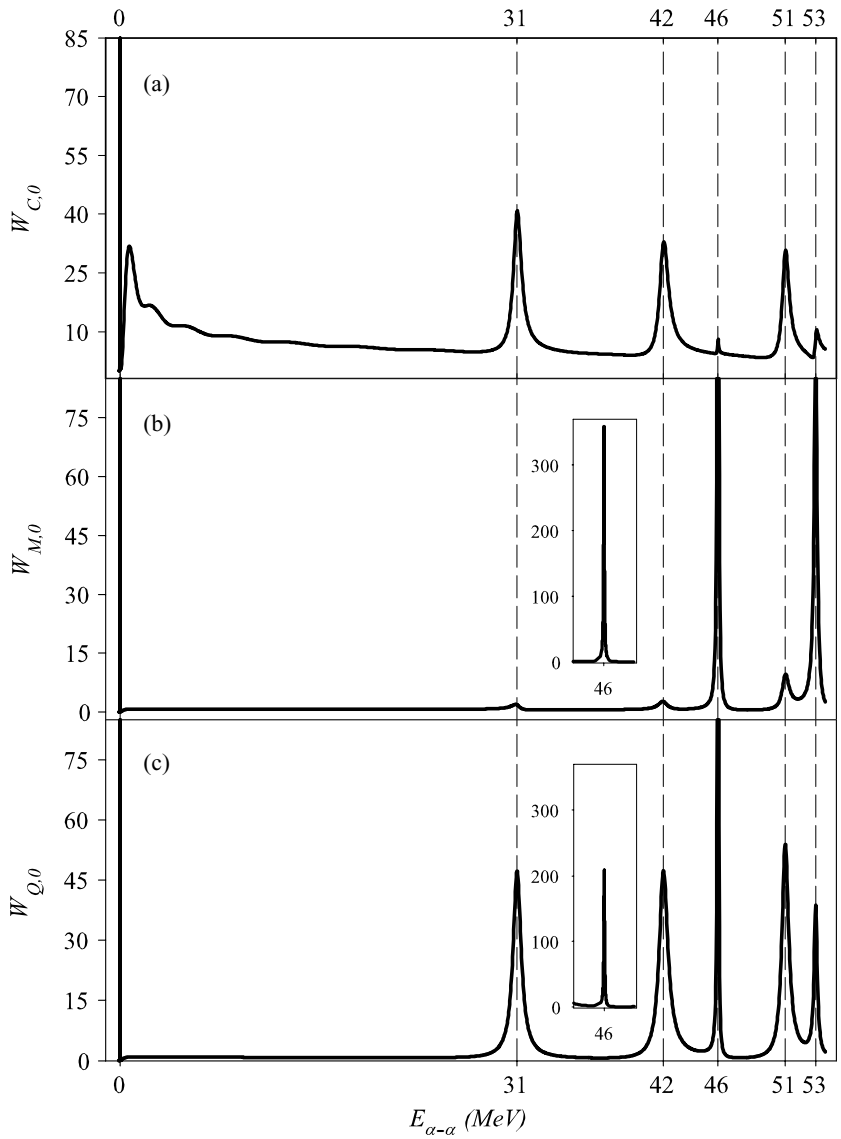

FIG. 3. $L = 0$ cluster (a), monopole (b), and quadrupole (c) channel weights obtained with the Volkov force. $E_{\alpha\text{-}\alpha}$ is the c.m. energy with respect to the cluster threshold. The panels in (b) and (c) show the weights in full scale for the resonance at 46 MeV.

the usual numerical way through

$$\frac{d^2\delta_l}{dE^2} = 0 \Longrightarrow E_r, \quad \Gamma = 2\left(\frac{d\delta_l}{dE}\bigg|_{E_r}\right)^{-1}. \tag{18}$$

We fix the common oscillator parameter b for the C, Q, and M expansion bases for each of the potentials so as to optimize an acceptable α-α threshold. These values can be found in Table I. We have also slightly modified the Majorana parameters of the Minnesota and modified Hasegawa-Nagata potentials to reproduce comparable values for the lowest $L = 0$, 2, and 4 resonances forming the ground-state rotational band in ^{8}Be; the values for the modified Majorana parameters are also shown in Table I. The table also contains the respective threshold energies for the three channels, which are obtained by fixing the asymptotic situation in each of the channels. For the α-α channel, it is naturally defined by letting the intercluster radius r tend to infinity: the threshold energy then amounts to twice the binding energy of the α particle, as no effective interaction component remains between both clusters. The definition of the threshold energies for the monopole and quadrupole channels is given in [33]. It is obtained by letting the respective collective coordinate tend to infinity. In the monopole case this is the spherical hyperradius of the eight-particle system: the threshold energy is then that of the eight free particles, i.e., no binding at all, or 0 MeV, as there is no effective interaction between any of the particles. In the quadrupole case, the collective coordinate extends along a single axis; when it goes to infinity, the effective interaction again is zero, and only a kinetic contribution, due to the forced polarization condition in the remaining two axial directions, remains.

In Fig. 1 we show the elastic α-α scattering $L = 0, 2,$ and 4 phase shifts within the energy region between the α-α and monopole thresholds as obtained from the full MJM calculations, including experimental data from [3] and [4]. The parameters of the calculation were chosen for convergent phase shifts, with $N = 50$ in (16) for the near interaction region and

TABLE III. Comparison of the resonance energies $E_{iL}^{\widetilde{MQ}}$ in the orthogonal complement to the cluster mode, denoted by $\widetilde{\mathrm{MQ}}$. All energies are in MeV. "Mode" stands for the content of the most prominent orthogonal monopole $\psi_{jL}^{\widetilde{M}}$ or quadrupole $\psi_{jL}^{\widetilde{Q}}$ eigenstates, in particular eigenstate $\psi_{iL}^{\widetilde{MQ}}$.

	Mi			V1			MHN		
	E_r	$E_{iL}^{\widetilde{\mathrm{MQ}}}$	Mode	E_r	$E_i^{\widetilde{\mathrm{MQ}}}$	Mode	E_r	$E_i^{\widetilde{\mathrm{MQ}}}$	Mode
0_2^+	34.78	32.02	92% $\widetilde{Q}_1$	30.51	29.90	95% $\widetilde{Q}_1$	33.78	33.13	97% $\widetilde{Q}_1$
0_3^+	44.45	44.19	75% $\widetilde{Q}_2$	41.72	41.52	90% $\widetilde{Q}_2$	46.04	45.73	89% $\widetilde{Q}_2$
0_4^+	48.41	48.31	56% $\widetilde{M}_1$	45.92	45.77	43% $\widetilde{M}_1$	51.42	51.15	66% $\widetilde{M}_1$
0_5^+	x	x	x	51.06	51.02	72% $\widetilde{Q}_3$	56.08	55.95	65% $\widetilde{Q}_3$
0_6^+	x	x	x	53.41	53.33	63% $\widetilde{M}_2$	x	x	x
2_2^+	35.12	34.33	90% $\widetilde{Q}_1$	32.59	31.96	94% $\widetilde{Q}_1$	36.08	35.38	96% $\widetilde{Q}_1$
2_3^+	46.51	46.21	66% $\widetilde{Q}_2$	43.48	43.27	93% $\widetilde{Q}_2$	47.90	47.60	89% $\widetilde{Q}_2$
2_4^+	47.17	47.17	58% $\widetilde{M}_1$	44.48	44.46	66% $\widetilde{M}_1$	49.69	49.59	71% $\widetilde{M}_1$
2_5^+	x	x	x	52.84	52.39	50% $\widetilde{Q}_3$	57.40	57.24	45% $\widetilde{Q}_3$
4_2^+	40.89	39.89	80% $\widetilde{Q}_1$	37.75	36.94	88% $\widetilde{Q}_1$	41.85	40.81	93% $\widetilde{Q}_1$
4_3^+	47.26	46.95	62% $\widetilde{M}_1$	44.17	43.84	71% $\widetilde{M}_1$	49.03	48.99	79% $\widetilde{M}_1$
4_4^+	x	x	x	48.01	47.59	87% $\widetilde{Q}_2$	52.64	51.98	92% $\widetilde{Q}_2$
4_5^+	x	x	x	53.68	53.60	86% $\widetilde{M}_2$	x	x	x

$M = 100$ for truncating the sum in (17) for all channels. The common states in the different channels for $n = 0$ have been taken into account properly, and forbidden Pauli states have been explicitly removed from the calculation.

One immediately recognizes from Fig. 1 the low-lying rotational structure of ^{8}Be. A rich resonance structure beyond 30 MeV above the cluster threshold appears through the coupling with the collective channels. This is made clear in Fig. 2, where the pure cluster phase shifts are compared to those of the fully coupled ones for V1 and $L = 0$. The effects are qualitatively well reproduced by all potentials considered, implying that the effect is a genuine one, independent of the specific choice of *NN* interaction. Table II lists the resonance parameters obtained from the phase shifts in Fig. 1 by applying (18).

IV. ANALYSIS

The results of the previous section indicate an important effect of the quadrupole and/or monopole deformation on the elastic α-α continuum. It manifests itself as relatively narrow resonances appearing above 30 MeV and below the thresholds of the collective modes.

To analyze these results, we examine the multichannel wave function for channel content by calculating channel weights:

$$W_{\upsilon,L} = \sum_n \left(c_{nL}^{\upsilon}\right)^2. \tag{19}$$

Figure 3 shows the channel weights for each of the three channels (α-α, monopole, and quadrupole) as a function of energy for V1 and $L = 0$. The figure includes the resonance positions for reference. This picture indicates the strong polarization effects at the resonance energies, emphasizing that the preferred configurations for ^{8}Be in the compound system at these resonance energies are dominated by the monopole and/or quadrupole modes. Even more, the collective resonances suggest a decoupled picture in the sense that each resonance is either essentially of a quadrupole or monopole nature. The 46 MeV resonance, shown in full scale in separate panels in Fig. 3, is split over the monopole and quadrupole modes, but it shows a predominance in the monopole channel. Keep in mind, however, that the channels are not orthogonal to each other, and that this fact blurs a clear-cut comparison.

To further analyze the results in terms of the collective modes, we suggest considering the orthogonal complement of the quadrupole and monopole bases with respect to the α channel. This effectively removes the nonorthogonality coupling between the α channel and the collective ones. We denote the resulting subspaces by $\widetilde{Q}$, $\widetilde{M}$, and $\widetilde{QM}$, when the coupled orthogonal complement is used. The transformed bases are easily obtained through Schmidt orthogonalization as

$$\begin{aligned}\psi_{nL}^{\widetilde{M}} &= \left[\psi_{nL}^{M} - \langle\psi_{nL}^{M}|\psi_{nL}^{C}\rangle\psi_{nL}^{C}\right]\Big/\sqrt{1-\langle\psi_{nL}^{M}|\psi_{nL}^{C}\rangle^2},\\ \psi_{nL}^{\widetilde{Q}} &= \left[\psi_{nL}^{Q} - \langle\psi_{nL}^{Q}|\psi_{nL}^{C}\rangle\psi_{nL}^{C}\right]\Big/\sqrt{1-\langle\psi_{nL}^{Q}|\psi_{nL}^{C}\rangle^2}.\end{aligned} \tag{20}$$

A further orthogonalization between the $\widetilde{Q}$ and $\widetilde{M}$ subspaces is not appropriate, as we will only be interested in either quadrupole or monopole contributions for the characterization of resonance states.

The multichannel Hilbert subspace is now separated into two nonoverlapping parts, the open α channel and the closed orthogonal collective components. This is similar to the Feshbach method [40] of projecting out the states of the "external" decay channel (the cluster one) at continuum energy E, and constructing the effective Hamiltonian in the "internal"

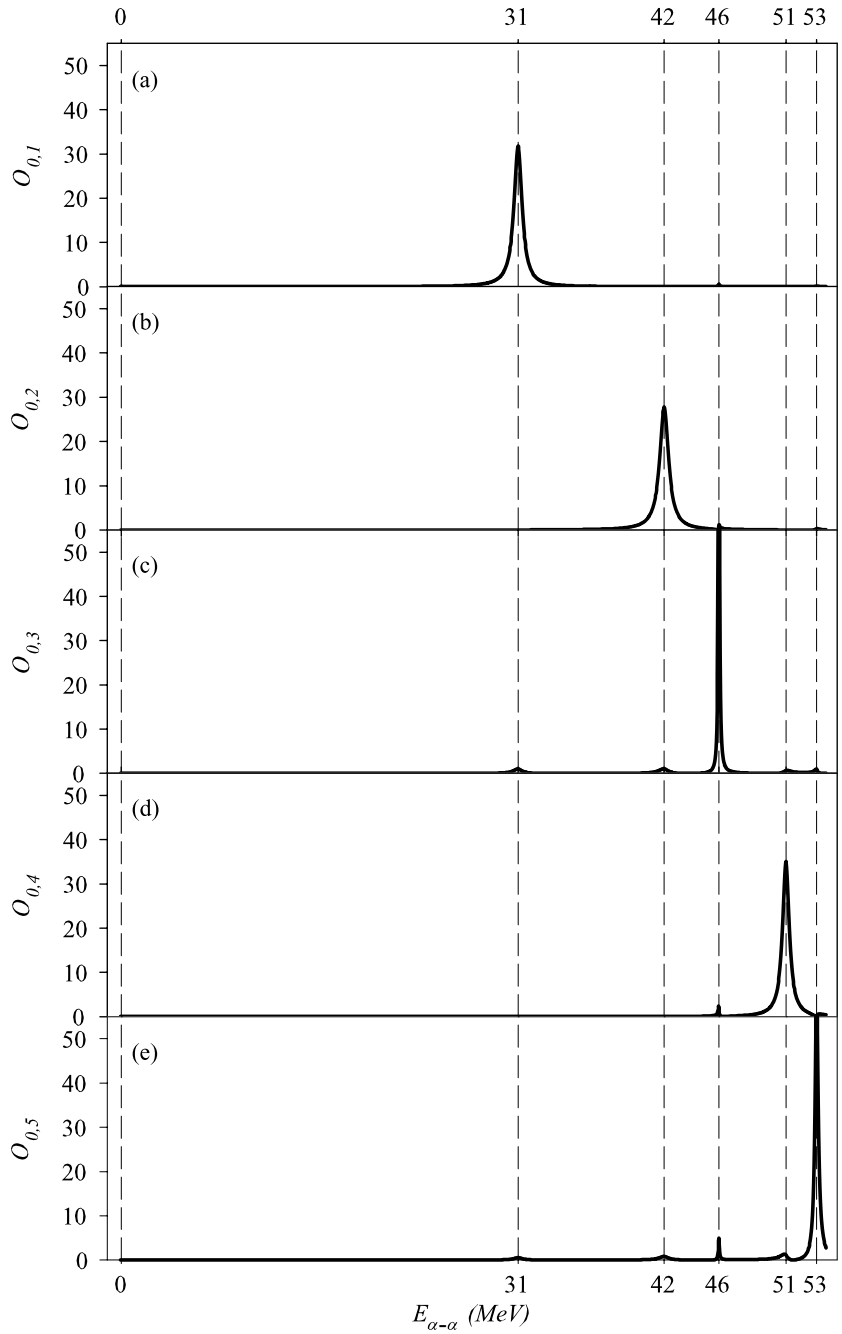

FIG. 4. Overlap of $L = 0$ energy wave function with the first (a), second (b), third (c), fourth (d), and fifth (e) eigenstates of the orthogonal complement to the cluster mode, calculated with the Volkov force. $E_{\alpha\text{-}\alpha}$ is the c.m. energy with respect to the cluster threshold.

space of many-body collective states. We calculate the bound eigenstates $E_{iL}^{\widetilde{MQ}}$ in the orthogonal to the cluster channel subspace and compare these to the resonance energies from the fully coupled scattering calculation. The results for all potentials are summarized in Table III. It is immediately apparent that the eigenenergies of the coupled orthogonal subspace correspond almost exactly to the resonance energies, except for the "ground-state" one which can be completely attributed to the Coulomb barrier in the α-α configuration. In Fig. 4, we show for V1 and $L = 0$ the content of the energy wave function in terms of the eigenstates of the orthogonal complement $O_{L,j} = \langle \psi_L^E | \psi_{jL}^{\widetilde{MQ}} \rangle^2$. It confirms the one-to-one correspondence of the resonances to the orthogonal complement eigenstates.

A final aspect to be studied is the specific polarization nature of the resonances suggested by Fig. 4. To this end, we calculate separately the spectrum in both the $\widetilde{Q}$ and $\widetilde{M}$ spaces. The combination of these uncoupled spectra is comparable to the coupled $\widetilde{Q}$ and $\widetilde{M}$ diagonalization, indicating a limited dynamical coupling between both subspaces. We indicate this in Table III by showing for each eigenstate of the coupled orthogonal complement the content $\langle \psi_{iL}^{\widetilde{MQ}} | \psi_{jL}^{\widetilde{M}} \rangle^2$ or $\langle \psi_{iL}^{\widetilde{MQ}} | \psi_{jL}^{\widetilde{Q}} \rangle^2$ of the most prominent uncoupled eigenstate. This confirms in most cases an almost pure polarization mode for

each coupled eigenstate and thus the corresponding resonance. These results are seen to be qualitatively identical for all three potentials considered in this work and for all $L = 0, 2$, and 4 values.

From Table III, one notices that the energy of the resonance states lies above the corresponding eigenenergy of the collective orthogonal complement. This confirms the results of Ref. [41], where it was shown that the coupling between orthogonal open and closed channels transforms the bound state from the closed channel into a resonance with an energy above the bound-state one. Table III also indicates a rotational behavior for the quadrupole-related resonances, closely following an $L(L + 1)$ energy spacing, whereas the monopole-related resonances remain roughly at the same energy.

V. CONCLUSIONS

We have presented the results for the elastic α-α spectrum for ^{8}Be obtained from a calculation in which the α-cluster configuration is coupled to the collective Sp(2,R) quadrupole and monopole modes. The energy range considered is between the α-channel and the monopole (full eight-particle decay) thresholds. To accommodate both the open α channel and the closed collective channels, we considered a multichannel version of the modified J-matrix method.

The results indicate, apart from the well-known low-lying rotational band attributed to Coulomb repulsion in the α-α description, a rich spectrum of relatively narrow resonances above 30 MeV. We have shown that the resonances are connected to the eigenstates of the collective subspace, orthogonalized to the open α channel. More specifically, we have shown that the resonances are essentially of quadrupole or monopole nature and thus exhibit a specific polarization of the nucleus. This indicates that both the quadrupole and monopole eigenmodes remain mainly uncoupled, as shown earlier [14] for bound *sd*-nuclei. It shows that both collective symmetries are important in the compound eight-particle system at specific energies in α-α scattering.

ACKNOWLEDGMENTS

The authors A. Sytcheva and V. S. Vasilevsky are grateful to the Department of Mathematics and Computer Science of the University of Antwerp for its hospitality. All authors acknowledge the financial support from the FWO-Vlaanderen.

[1] F. Ajzenberg-Selove, Nucl. Phys. **A490**, 1 (1988).
[2] D. Tilley, J. Kelley, J. Godwin, D. Millener, J. Purcell, C. Sheu, and H. Weller, Nucl. Phys. **A745**, 155 (2004).
[3] A. D. Bacher, F. Resmini, H. Conzett, R. de Swiniarski, H. Meiner, and J. Ernst, Phys. Rev. Lett. **29**, 1331 (1972).
[4] P. Darriulat, G. Igo, H. Pugh, and H. Holmgren, Phys. Rev. **137**, 315 (1965).
[5] N. Arena, I. Barit, S. Cavallaro, A. D'Arrigo, G. Fazio, and G. Giardina, J. Phys. G **20**, 1973 (1994).
[6] K. Wildermuth and Y. Tang, *A Unified Theory of the Nucleus* (Vieweg, Braunschweig, 1977).
[7] Y. C. Tang, Microscopic Description of the Nuclear Cluster Theory, in *Lecture Notes in Physics* (Springer, Berlin, 1981), Vol. 145 [As it was mentioned in Phys. Rev. C **25**, 2902 (1982)].
[8] Y. C. Tang, M. LeMere, and D. R. Thompson, Phys. Rep. **47**, 167 (1978).
[9] J. Wheeler, Phys. Rev. **52**, 1083 (1937).
[10] D. Hill and J. Wheeler, Phys. Rev. **89**, 1102 (1953).
[11] S. Saito, Prog. Theor. Phys. (Suppl.) **62**, 11 (1977).
[12] K. Arai and A. T. Kruppa, Phys. Rev. C **60**, 064315 (1999).
[13] J. Humblet, A. Csótó, and K. Langanke, Nucl. Phys. **A638**, 714 (1998).
[14] F. Arickx, J. Broeckhove, E. Caurier, and P. Van Leuven, Nucl. Phys. **A398**, 467 (1982).
[15] F. Arickx, J. Broeckhove, and E. Deumens, Nucl. Phys. **A269**, 318 (1979).
[16] F. Arickx, Nucl. Phys. **A284**, 264 (1977).
[17] D. Rowe, Rep. Prog. Phys. **48**, 1419 (1985).
[18] Y. Suzuki, Prog. Theor. Phys. **75**, 1377 (1986).
[19] K. Hecht and D. Braunschweig, Nucl. Phys. **A295**, 34 (1978).
[20] G. Filippov, V. Vasilevsky, and A. Nesterov, Nucl. Phys. **A426**, 327 (1984).
[21] G. Filippov, Revista Nuovo Cimento **12**, 1 (1989).
[22] G. Filippov, V. Vasilevsky, S. Kruchinin, and L. Chopovsky, Sov. J. Nucl. Phys. **43**, 536 (1986).
[23] E. Deumens, Nucl. Phys. **A423**, 52 (1984).
[24] D. Baye and M. Kruglanski, Phys. Rev. C **45**, 1321 (1992).
[25] W. Vanroose, J. Broeckhove, and F. Arickx, Phys. Rev. Lett. **88**, 10404 (2002).
[26] J. Broeckhove, F. Arickx, W. Vanroose, and V. Vasilevsky, J. Phys. A **37**, 7769 (2004).
[27] E. J. Heller and H. A. Yamani, Phys. Rev. A **9**, 1201 (1974).
[28] F. Arickx, J. Broeckhove, P. Van Leuven, V. Vasilevsky, and G. Filippov, Am. J. Phys. **62**, 362 (1994).
[29] V. Vasilevsky and F. Arickx, Phys. Rev. A **55**, 265 (1997).
[30] A. Volkov, Nucl. Phys. **74**, 33 (1965).
[31] D. Thompson, M. LeMere, and Y. Tang, Nucl. Phys. **A286**, 53 (1977).
[32] F. Tanabe, A. Tohsaki, and R. Tamagaki, Prog. Theor. Phys. **53**, 677 (1975).
[33] V. Vasilevsky, G. Filippov, F. Arickx, J. Broeckhove, and P. Van Leuven, J. Phys. G **18**, 1227 (1992).
[34] V. Vasilevsky, A. Nesterov, F. Arickx, and P. Van Leuven, Phys. Atom. Nuclei **60**, 343 (1997).
[35] V. Vasilevsky, A. Nesterov, F. Arickx, and J. Broeckhove, Phys. Rev. C **63**, 034606 (2001).
[36] V. Vasilevsky, A. Nesterov, F. Arickx, and J. Broeckhove, Phys. Rev. C **63**, 034607 (2001).
[37] F. Arickx, J. Broeckhove, A. Nesterov, V. Vasilvesky, and W. Vanroose, in *J-Matrix Method and Its Applications*, edited by A. Alhaidari (Nova Science Publishers, New York, in press).
[38] A. Hasegawa and S. Nagata, Prog. Theor. Phys. **38**, 118 (1967).

[39] A. Hasegawa and S. Nagata, Prog. Theor. Phys. **45**, 1786 (1971).
[40] H. Feshbach, *Theoretical Nuclear Physics. Nuclear Reactions* (Wiley-Interscience, New York, 1991).
[41] F. Arickx, J. Broeckhove, W. Vanroose, P. Van Leuven, and V. Vasilevsky, in *Proceedings of the 6th International Spring Seminar in Nuclear Physics, "Highlights of Modern Nuclear Structure*," St. Agata, Italy, May 1998, edited by A. Covello (World Scientific, Singapore, 1998), 485.